International Journal of Automotive Technology, Vol. 23, No. 6, pp. 1673–1680 (2022)
DOI 10.1007/s12239–022–0145–4

pISSN 1229–9138/ eISSN 1976–3832

PLATOONING AND BASE FLAPS FOR DRAG REDUCTION OF TRUCKS

Christian Navid Nayeri* and Hanns-Joachim Schmidt

Hermann-Föttinger-Institute, Technische Universität Berlin, Berlin 10623, Germany

(Received 30 November 2020; Revised 30 June 2021; Accepted 18 April 2022)

ABSTRACT–Experimental investigations on generic truck models were carried out on the combined drag reducing effects of platooning and base flaps. A towing tank facility was used with model scales of 1:15 and Reynolds numbers of up to 10^6. Two vehicle and three vehicle configurations with variable intervehicle distances were analyzed without considering the influence of a ground proximity. The potential of two and three vehicle platoons for drag reduction is clearly demonstrated exemplary for flap angles of 15°. Under certain conditions base flaps increase these benefits. However, their effect depends on the intervehicle distance, the flap angle, and the vehicle position within the platoon. The platoon drag can be reduced by additional 25 % when base flaps are added which corresponds to an overall platoon drag reduction of about 40 %.

KEY WORDS : Aerodynamics, Flow control, Towing tank, Truck, Platoon, Convoy

NOMENCLATURE

A	: frontal vehicle area, m^2
C_d	: drag coefficient, []
c_p	: pressure coefficient, []
d	: distance normalized with sqrt(A), []
α	: base flap deflection angle, °

1. INTRODUCTION

Heavy vehicles such as tractor trailers or buses have a large aerodynamic drag resulting in high fuel consumption. Base flaps or boat tails are well known add-on devices to reduce the drag created through separation at the rear of such vehicles. Another measure for drag reduction are platoons. Trucks driving in a platoon consume less fuel as the overall drag is reduced through the slipstream effect.

In the present work the combined effect of platooning and base flaps are investigated systematically in a towing tank. The configurations include two and three vehicles with intervehicle distances varying from 0.25 to 4.25 normalized vehicle heights. In order to keep the investigations more general the flow around the models is not restricted, i.e. the effect of ground proximity is not considered.

In the following a brief review on base flaps, platoons, and towing tanks is given.

1.1. Base Flaps

In order to accomplish drag reduction at the rear end of tractor-trailers various passive methods have been explored over the past decades. Mason and Beebe (1978) obtained a drag reduction of 5 % using a “non-ventilated cavity design”. Bilanin (1985) filed a patent in 1985 on a variation of this cavity design concept that insets the endplates from the trailer perimeter. Filed patents by Boivin and Roberge (2001) describe an attachment of plates to the edge of the trailer and inclination toward the centerline (so-called base flaps), but without a bottom plate. The extensive parameter study performed by Cooper (1985) on several bluff body models having the shape of a heavy vehicle demonstrates that those straight flaps perform slightly better than curved flaps. However, it was shown that there is no benefit in having flaps longer than about 25 % of the truck width and that there is an optimum flap angle beyond which the drag savings begin to diminish due to flow separation over the flap. He determined an optimum flap angle of 15° and a drag reduction of 7 ~ 10 %. Göhring and Krämer (1991) as well as Porth and Krämer (1991), and the same team, Porth and Krämer (1993) conducted road tests on an original European heavy-class tractor-semitrailer combination and also wind tunnel tests on a 1/2.5-scale model. Base flaps exhibited a drag reduction of 7 ~ 11 %. The authors concluded that an increased flap length leads to higher reductions in drag and that each flap length has an optimum flap tilt angle with regard to the maximum drag reduction. Beyond these flap angles the flow separates and the drag increases significantly.

Browand *et al*. (2005) investigated the effect of base flaps with different deflection angles at full-scale Reynolds numbers. It was stated that flaps inclined by 13° provide the highest reduction in drag and that base flaps at all angles of yaw provide better results than boat-tail plates. These observations make base flaps suitable for commercial

**Corresponding author*. e-mail: christian.nayeri@tu-berlin.de

utilization, which has motivated companies to commercialize this kind of device in recent years (Betterflow, 2020; Wabash National, 2020; WABCO, 2020).

1.2. Platooning

Several early studies (e.g., Koenig and Roshko, 1985; Hoerner, 1965; Gu, 1996) demonstrate the potential for drag reduction and the underlying flow effects of subsequently aligning bodies. The beneficial effect is primarily due to the shielding effect which reduces the stagnation pressure $c_{p\text{–}stagnation} = u^2/2\rho$ at the front of the trailing body at very short distances.

The fluid mechanical interaction of those bodies has gained increasing relevance in the commercial transportation sector because it enables a significant reduction of the aerodynamic drag of vehicles arranged in a platoon. Therefore, numerous studies aim on the effectiveness of platooning for various more or less realistic vehicle models to determine the most effective platooning constellations.

Bonnet and Fritz (2000) considered the fuel consumption savings of two closely spaced, coupled heavy-duty trucks on a test track. The spacing is varied between 6 and 16 meters. The largest benefit was obtained for a distance of 10 meters and a velocity of 80 km/h. The fuel consumption of the trail and the lead truck was reduced up to 21 % and 7 %, respectively. Lammert *et al*. (2014) achieved an averaged fuel reduction of < 5.3 % for the leading and < 9.7 % for the trailing vehicle whereas Tsugawa *et al*. (2011) achieved about 14 % for a platoon of three trucks under similar conditions. Browand *et al*. (2004) observed a drag reduction of 15 ~ 20 % with realistic truck models at a full-scale distance of about 6 m within the wind tunnel and 8 ~ 11 % fuel reduction at full-scale test (Göhring and Krämer, 1991). The effect of front geometry changes is impressively shown by Hammache and Browand (2004) and Hammache *et al.* (2002). The comparison of wind tunnel and field tests reveal significant deviations (Watkins *et al.*, 1993) which may be attributed to Reynolds number effects and varying boundary conditions (e.g., stationary wind tunnel grounds, turbulence intensity). Other recent studies on platooning of realistic truck geometries are McAuliffe and Ahmadi-Baloutaki (2018) and Törnell *et al*. (2021).

1.3. Base Flaps and Platoons

A direct comparison of both measures, base flaps and platooning, is made by Browand *et al*. (2004) They conclude that the average fuel savings obtained with platooning are higher than achieved with a single truck equipped with base flaps. Two numerical theses were examined at the TU Delft considering the influence of base flaps on a platoon of three generic truck models. A coarse modulation of the flap angle, the front radius, and the vehicle distance were examined by Gheyssens (2016) and Doppenberg (2015). Base flaps attached to a specific vehicle mainly influence subsequent vehicles. With increasing flap angle the base pressure of the leading model and the frontal stagnation pressure of the trailing model increase. As a consequence, the drag of the leading vehicle decreases whereas the drag of the trailing model increases. Which of these two effects is larger concerning the mean drag of the platoon depends on the vehicle distance, the flap angle, and the front edge radius. The lowest absolute platoon drag is observed when all vehicles are equipped with 12° deflected flaps.

Although platooning appears to have a high potential for fuel saving it remains challenging to develop technologies which overcome the logistic and infrastructural barriers. This circumstance motivates several research groups to realize suitable solutions for autonomous road traffic (e.g., PATH project, 2016; KONVOI project, 2016; European truck challenge, 2016). A general overview on the outcomes of most of these projects is provided by Patten *et al*. (2012).

The current experimental study represents a continuation of these studies. A platoon of generic truck models equipped with base flaps is investigated in a large towing tank. In contrast to most of the other studies, the effect of ground proximity is not considered for the sake of simplicity.

1.4. Towing Tank Experiments

A first general overview on the advantages and disadvantages of towing tank experiments is provided by Gad-el Hak (1987). Several publications focus on the aerodynamics of vehicle-shaped models. Larsson *et al*. (1989) investigated a full-scale passenger car in a towing tank and a wind tunnel to demonstrate the feasibility and practicability of experiments in water. Jönsson *et al*. (2014) inspected the underfloor flow field of a train model in a water towing tank by the use of particle image velocimetry (PIV). Nayeri *et al*. (2016) compared wind tunnel and towing tank experiments with a single box-shaped model in combination with passive flow control via base flaps. The drag improvements of various flap angle configurations reveal a good agreement between the facilities. The experimental study of Schmidt *et al*. (2018) represents a continuation of this work. They demonstrate that the results with a bluff body model equipped with active and passive flow control in water and the actuation methods can be completely transferred between the working fluids.

2. EXPERIMENTAL SETUP

The experiments are conducted in the large towing tank facility of the Technische Universität Berlin (Figure 1), which has an overall length of 250 m, a width of 8.1 m, and an average depth of 4.8 m. The test objects are mounted to a towing carriage, which travels at computer-controlled velocities along the tank. At maximum velocity, a Reynolds number of 12 × 10^6 per meter characteristic length scale is achievable. The relative velocity between model and quiescent environment corresponds to the carriage velocity

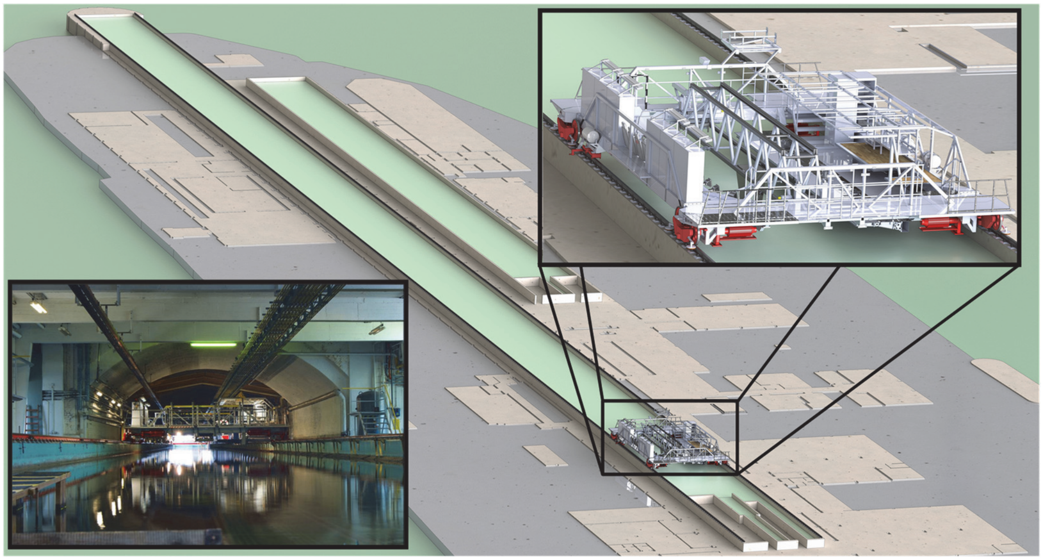

Figure 1. Towing tank and towing carriage at Technische Universität Berlin.

U_{model}. The towing carriage contains a measurement platform made from welded stainless-steel beams. Additional loads of 2 tons can be attached to this framework. It is traversable in vertical and lateral direction, which enables a continuous adjustment of the models' submergence depth.

2.1. Model and Mounting

The so-called GETS (General European Transport System) model is used in this study. This bluff body model represents a standard truck-trailer combination without any geometric details such as mirrors, wheels, or the gap between truck and trailer. This model geometry has been subject to several experimental and numerical studies (Schmidt *et al*., 2015; Schmidt *et al*., 2016; Schmidt *et al*., 2018; Doppenberg, 2015; Gheyssens, 2016) and therefore provides a sufficiently large database for comparison. Compared to previous experimental studies with a 10 % scaled model, the current models are downscaled to 1/15 full-scale to fit an entire three vehicle platoon to the measurement platform of the towing carriage. The resulting model dimensions are (L_{model} × W × H) = (1184 mm × 187 mm × 246 mm). The towing tank's cross-section results in a blockage of less than 1 %. The models' front edges are rounded with a radius of 35 mm and equipped with tripping tape to inhibit laminar separation. The bluff body models are additionally equipped with base flaps. These passive add-on devices are beneficial for drag reduction of trucks. The base flaps are mounted flush with the rear edges of the models. The flap inclination angle α is varied in this study in the range of $0° \leq \alpha \leq 20°$. The flap length is set to l_{flap} = 67 mm according to previous studies (Schmidt *et al*., 2015; Schmidt *et al*., 2016; Hoffmann *et al*., 2015) which corresponds to a full-scale flap length of 1 m and to 0.46 normalized distance *d* (*d* is defined by distance/sqrt(*A*)).

Figure 2. Photograph of the three model platoon configuration.

2.2. Measurement Equipment and Test Procedure

The velocity of the towing carriage is determined by a cyclometer, which generates a velocity equivalent TTL-signal with a resolution of 10,000 ticks per meter. A WAS4 pro Freq frequency to voltage converter from Weidmüller provides the analog velocity signal which is recorded simultaneously with the pressure and force data. The hydrodynamic drag forces acting on each model are measured with four one-component sensors KD140 in combination with GSV-1A8USB and GSV1A4 amplifiers by ME-Messsysteme. The sensor electronics are sealed with silicone. Each sensor has a measurement accuracy of ± 0.1 % full scale and an applicable range of 100 N. The force sensors are positioned within the model to measure only the streamwise force component (Figure 3). The alignment of the force sensors ensures the rigid connection to the mounting, which minimizes flow induced model oscillations.

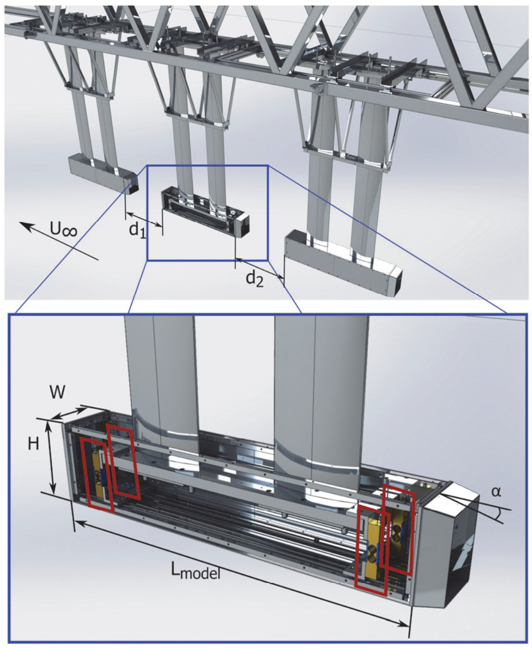

Figure 3. Platooning setup: Upper image shows how the GETS models are connected to the towing carriage; The image shows also the intervehicle distances; Bottom image shows the internal setup where the red rectangles highlight the four force sensors. Also, the base flap angle α is shown.

Differential pressure sensors are positioned within the models. These sensors are connected to pressure taps at the model surface for the determination of the static surface pressure. Although a number of pressure taps were implemented in the models, for the current analysis only those located in the center of the front and base of both bodies are used in this paper. The other taps did not provide any additional insight into the flow physics and should be distributed differently for future studies. Capacitative differential pressure sensors (26PC Series by Honeywell and HMU Series by FirstSensor AG) with 0.375 and 1 bar full range and a measurement error ± 0.2 % full-scale are used. The pressure sensors are coated in epoxy resin to make them waterproof. The reference pressure is obtained from a closed external reference volume outside the water tank.

The simultaneous acquisition of the freestream velocity, the pressure data, and the hydrodynamic drag forces is provided by the data acquisition system which consists of two synchronized cDAQs NI 9188. Due to the modification of the measurement hardware, the pressure and force measurement systems are calibrated prior and after the experiments. The measurement data are captured at a frame rate of 4 kHz. The effective measurement time is set to 10 seconds for each measurement configuration. Therefore, a single test run contains different Reynolds numbers by varying the carriage velocity. A settling time of 30 minutes between the test runs ensured quiescent water conditions in the towing tank.

3. RESULTS

The following chapter focusses on the platoon results. Section 3.1 describes the results obtained with the platoon of two vehicles (tandem) and section 3.2 with three vehicles and the influence of the rear end modifications.

In the graphs the measured drag coefficients are shown for each vehicle in the platoon: blue lines indicate the leading and red lines the trailing one. The drag coefficients are normalized by the drag coefficient of a single (isolated) model in baseline configuration, i.e. without any rear modification (base flaps):

$$C_{D_{normalized}} = \frac{C_{D,platoon}}{C_{D,single,baseline}}$$

The graphs also include the normalized averaged drag coefficient of the complete platoon as dashed lines. It is defined as:

$$C_{D_{platoon,normalized}} = \frac{1}{n}\sum_{i=1}^{n} \frac{C_{D,platoon,i}}{C_{D,single,baseline}}$$

3.1. Two Vehicle Configurations

The influence of the intervehicle distance d on the drag and base pressure for the two vehicle (tandem) configuration is shown in Figure 4.

Somewhat surprisingly the graph shows that the drag of the second vehicle is larger than that of the first. This is counterintuitive as one would expect that the second vehicle would benefit from the shielding effect of the first vehicle. However, a similar behavior was also reported by Hammache *et al.* (2002). He found that in a tandem configuration of simplified truck models (parallelepiped) rounded front edges lead to this counterintuitive behavior for normalized distances larger than 0.8 which he calls “weak interaction region”. This indicates that the geometry of the front edges of the trailing vehicles have a strong influence on the flow and thus on the pressure distribution in the gap.

In ongoing numerical simulations using DES the authors of this paper reproduced this exceptional behavior, i.e. the trailing vehicle having a larger drag than the leading one. These CFD studies will help to clarify the origin of this behavior and will be published later.

Four distinct interference zones can be identified: near, transitional, developed and reversion. The near zone ranges from d = 0.25 to 0.5 and shows a maximum drag reduction of about 50 % and 25 % for the leading and rear model,

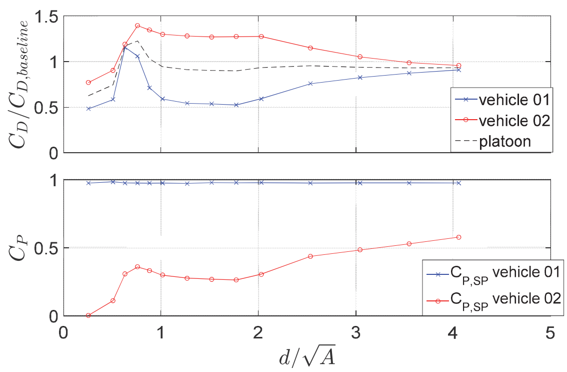

Figure 4. Baseline tandem configuration: Drag and pressure versus distance.

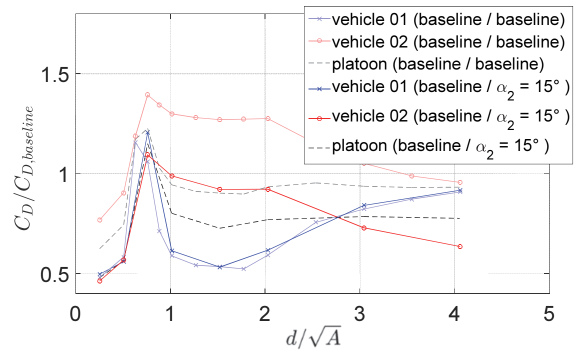

Figure 5. Two vehicles configurations: Second vehicle with base flaps. The legend (baseline/baseline) indicates that the first vehicle and the second vehicle are in baseline configuration. (baseline/α_2 = 15°) indicates that the first vehicle is in baseline configuration and the second vehicle is equipped with base flaps.

respectively. In the subsequent transitional zone from *d* =0.5 to 1.0 the drag of both vehicles increases drastically forming a distinct peak for the leading model at *d* ≈ 0.6 and a jump to a higher drag level of 125 % for the rear model at *d* ≈ 0.7. The origin of this peak cannot be explained yet. As the authors have not found a similar behavior in the literature, it is assumed that some particularity of the experimental setup might be the cause, e.g. oscillation of the models at short distances. This phenomenon is also subject of the abovementioned ongoing numerical simulations.

In the developed zone from *d* ≈ 1.0 to 2 the drag of the models remains almost constant with a larger drag for the second model of about 125 % and a much lower drag of about 50 % for the first model. Beyond *d* = 2.0 the drag values converge as expected to $C_{D_{normalized}} = 1$ of a single vehicle showing that the platoon effect diminishes.

The optimal overall platoon drag of 90 % is obtained in the developed zone.

It is worth mentioning that the measured drag coefficient of a single model is $C_d = 0.3$ which also corresponds to the values of a 1/10 scaled GETS-model measured in a wind tunnel and also towing tank (Schmidt *et al.*, 2016) (this drag is lower than for the case with ground effect $C_d = 0.36$ (Schmidt *et al.*, 2015)).

Figure 4 also shows the static pressure at the center of the front of the vehicles. The leading vehicle's stagnation pressure remains unaffected by the changes of vehicle distance whereas at the front of the trailing vehicle it reaches a minimum value of $c_p = 0$ at *d* = 0.25 (near zone). This low value not only contributes to the lowest drag of the second vehicle but also to a low drag of the leading vehicle as its base pressure is increased compared to the single vehicle value of -0.15. However, the pressure shown in the graph does not provide any insight on the cause of the drag peaks in the transition zone and why the second vehicle has always a higher drag compared to the single vehicle case and to vehicle 1 in the developed and reversion zones.

3.1.1. Two vehicles configurations: Second vehicle with base flaps

The effect of the base flaps on the drag of a single vehicle was studied for flap angles from 0 to 20° (not shown here). The results revealed that the flaps can reduce the drag by more than 30 % with the optimum angle being α_2 = 15°. For flap angles larger than 15° the drag increases again most probably due to flow separation confirming former results (Hoffmann *et al.*, 2015).

A configuration where only the second vehicle is equipped with 15° base flaps was investigated is shown in Figure 5. The plot shows that the leading vehicle has the same behavior as in the baseline case (blue lines). However, the rear vehicle experiences an important and constant drag reduction of almost 50 % compared to its baseline tandem configuration (note the $\Delta C_{D_{normalized}}$ ≈0.5 between the red lines). In the developed zone (d ≈ 1.0 to 2) the drag of the second vehicle is lower than its baseline drag in tandem configuration.

This effect was also obtained for other flaps angles (not shown here). The platoon drag for this configuration is as low as 80 % of the baseline value except for the transitional zone where it has a peak value of 120 %.

3.1.2. Two vehicles configurations: Both vehicles with base flaps

The tandem configuration with both vehicles equipped with 15° base flaps is presented in Figure 6. Here the most obvious change is that vehicle one does not exhibit a drag peak in the transitional zone but shows a rather linear increase from a drag minimum ($C_{D_{normalized}}$=0) at the smallest distance investigated to the single vehicle drag value with increasing distance. The drag behavior of the second vehicle remains qualitatively similar compared to the configuration where it is the only vehicle with base

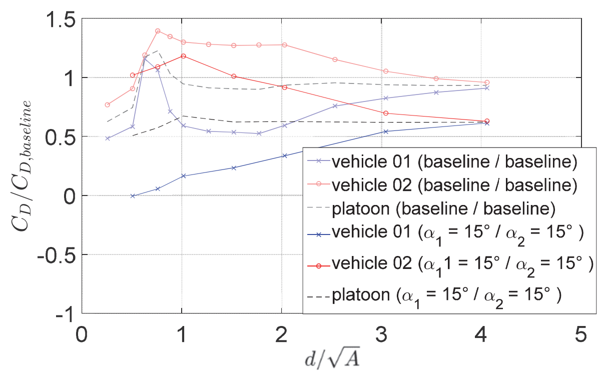

Figure 6. Two vehicles configurations: Both vehicles with base flaps (and for comparison without base flaps).

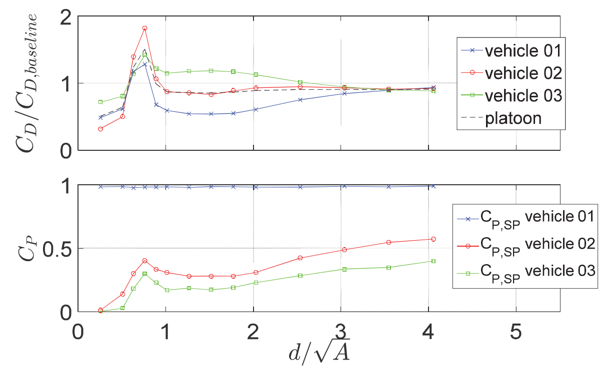

Figure 7. Three vehicle platoon: Effect of vehicle distance on drag without base flaps.

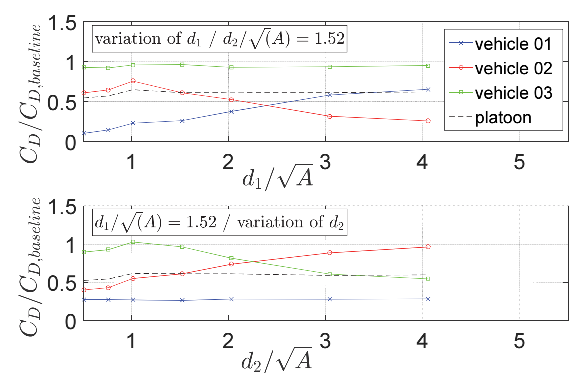

Figure 8. Three vehicle platoons with $\alpha_{1/2/3}$ = 15°: Top, variation of first distance d_1; Bottom, Variation of d_2.

flaps. Its normalized drag decreases from a maximum value $C_{D_{normalized}} \approx 1.2$ at $d \approx 1.0$ to about 0.6 at $d \approx 4.0$. The overall platoon drag remains quite constant for all investigated distances and is much lower that the abovementioned configurations having only 60 % of the baseline drag. Thus, it can be stated that base flaps in combination with a tandem platoon provide a larger drag reduction potential as each individual measure alone.

3.2. Three Vehicles Configurations

When adding a third model to the tandem configuration we obtain a three vehicle platoon (Figure 3). Figure 7 illustrates the drag and pressure changes for simultaneous variation of distances d_1 and d_2 of the baseline vehicles. Similar to the tandem case we can identify four regions: near, transitional, developed, and reversion. In the first zone ($d_{1/2}$ = 0.25 ~ 0.5) all vehicles exhibit their lowest drag compared to the reference case. Here, obviously the low stagnation pressures at the front result in a significant drag reduction for vehicles two and three. Furthermore, the stagnation pressure of vehicle two increases the base pressure of the first vehicle from c_p = -0.15 to 0 resulting in a lower drag coefficient for the leading vehicle. In zone two ($d_{1/2}$ = 0.5 to 1.0) a maximum drag peak is obtained with the largest value of c_D = 1.8 for vehicle two. In the tandem case also the second vehicle exhibited the highest peak but 40 % lower (c_D = 1.4) than in the three vehicle configuration. The developed region ($d_{1/2}$ = 1.0 ~ 2.0) shows drag reductions of vehicles one and two of about 50 % and 20 %, respectively. Surprisingly, it is not the second vehicle which benefits most from the platoon. The rear vehicle has a drag increase of about 20 % as it was also found in the tandem case.

The overall platoon drag behaves qualitatively similar to the tandem case with a maximal drag reduction of about 15 % for $d_{1/2}$=1.0-2.0.

In summary it can be stated that for the three vehicle configuration the drag behavior of the first and last vehicle corresponds to the leading and rear vehicle of the tandem configuration. Presumably, because the flow field in the gaps between the models are similar, and the effects of the gaps cancel out each other. Therefore, the drag of vehicle 2 corresponds quite well with the tandem platoon drag.

Next, we consider the effect of base flaps (α = 15°) in a three vehicle platoon. Figure 8 shows the drag values for one intervehicle distance kept constant while the other is varied. The fixed distance was set to d = 1.5 because it is in the middle of the developed zone ($d_{1/2}$ = 1.0 ~ 2.0) and provides the lowest drag in all vehicle constellations. In the case where d_1 is varied (Figure 8, top) and d_2 is kept constant the first vehicle shows a similar trend as in the tandem case having a minimum drag at the smallest distance and an almost linearly increasing drag with increasing distance d_1. The relative drag reduction for this vehicle is also of similar magnitude. In contrast to the first vehicle, the second one experiences an important drag reduction of about 40 % compared to the tandem case for all d_1. The qualitative graph profile of the drag to distance relationship of the second vehicle corresponds also well to the tandem case. Even the drag peak at $d_1 = 1$ is reproduced. Not surprisingly, the third vehicle has an almost constant drag reduction of about 8 % as its distance is not varying. The overall platoon drag remains quasi unchanged for all d_1 variations at about 60 % of the baseline case which is about the same as for the two vehicle configuration.

The configuration for varying d_2 but constant d_1 is depicted in Figure 8 (bottom). The first vehicle's drag remains constant at a very low value of 25 % of the baseline drag. Vehicle 2 and 3 behave qualitatively similar to the vehicles 1 and 2, respectively, of the case with constant d_2. However, their drag reduction is roughly 20 to 40 % lower as in the other case. Although the individual drag reductions change drastically compared to the constant d_2 case, the overall drag reduction remains at about 60 % of the baseline case. This corresponds to the benefit of the tandem configuration indicating that a three vehicle configuration with base flaps does not outperform a tandem configuration in terms of fuel saving potential.

4. CONCLUSION

The potential of two and three generic vehicle platoons for drag reduction is clearly demonstrated. Under certain conditions base flaps increase these benefits. However, their effect depends on the intervehicle distance, the flap angle, and the vehicle position within the platoon. The results of the three vehicle configurations don't indicate an additional drag reduction compared to the tandem configuration (e.g., the baseline platoon drag). However, the underlying flow physics need to be clarified more in detail for some unexpected findings. For example, the evolution of the rear model drag seems to be highly affected by the gap flow in front of the model and also by its front shape, i.e. rounded edges. Further studies are underway using DES numerical simulation to identify the origins of these behaviors.

It should be kept in mind that this study considers simplified geometries in platoon arrangement without any ground effect, thus the transfer of the results to realistic truck shapes in platoon configuration is not straightforward.

ACKNOWLEDGEMENT–The funding for the presented investigations was provided by the German Science Foundation (Deutsche Forschungsgemeinschaft). The authors also acknowledge for fruitful discussions with Lennart Löfdahl.

REFERENCES

Betterflow GmbH (2020). http://www.betterflow.com, Accessed on November 23, 2020.

Bilanin, A. J. (1985). Vehicle drag reducer. US Patent No. 4682808.

Boivin, M. and Roberge, K. (2001). Air drag reducing apparatus. US Patent No. 6257654.

Bonnet, C. and Fritz, H. (2000). Fuel consumption reduction in a platoon: Experimental results with two electronically coupled trucks at close spacing. *SAE Paper No*. 2000-01-3056.

Browand, F. and Hammache, M. (2004). The limits of drag behavior for two bluff bodies in tandem. *SAE Paper No*. 2004-01-1145.

Browand, F., McArthur, J. and Radovich, C. (2004). Fuel saving achieved in the field test of two tandem trucks. California Partners for Advanced Transit and Highways (PATH). Research Paper No. UCB-ITS-PRR-2004-20.

Browand, F., Radovich, C. and Boivin, M. (2005). Fuel savings by means of flaps attached to the base of a trailer: Field test results. *SAE Paper No*. 2005-01-1016.

Cooper, K. R. (1985). The effect of front-edge rounding and rear-edge shaping on the aerodynamic drag of bluff vehicles in ground proximity. *SAE Trans*., 727–757.

Doppenberg, S. P. (2015). *Drag Influence of Tails in a Platoon of Bluff Bodies*. M. S. Thesis. Delft University, Delft, The Netherlands.

European Truck Platooning Challenge (2016). https:// www. eutruckplatooning.com, Accessed on May 12, 2016.

Gad-el-Hak, M. (1987). The water towing tank as an experimental facility. *Experiments in Fluids* **5**, **5**, 289–297.

Gheyssens, T. (2016). *Aerodynamic Analysis of a Platoon of Bluff Bodies Subjected to Cross Wind, a Numerical Investigation on the Effect of Drag Reduction Devices*. Ph. D. Dissertation. Delft University, Delft, The Netherlands.

Göhring, E. and Krämer, W. (1991). Fahrwiderstandsreduzierende massnahmen zur weiteren optimierung der wirtschaftlichkeit von sattelzϋgen-teil 1. *Automobiltechnische Zeitschrift* **93**, **7/8**, 434–439.

Gu, Z. (1996). On interference between two circular cylinders at supercritical Reynolds number. *J. Wind Engineering and Industrial Aerodynamics* **62**, **2-3**, 175–190.

Hammache, M. and Browand, F. (2004). On the Aerodynamics of Tractor-Trailers. *The Aerodynamics of Heavy Vehicles: Trucks, Buses, and Trains* (pp. 185–205). Springer, Berlin, Heidelberg. Germany.

Hammache, M., Michaelian, M. and Browand, F. (2002). Aerodynamic forces on truck models, including two trucks in tandem. California Partners for Advanced Transit and Highways (PATH). Research Paper No. UCB-ITS-PRR-2007-27.

Hoerner, S. F. (1965). *Fluid-Dynamic Drag*. Hoerner Fluid Dynamics. Brick Town, New Jersey, USA.

Hoffmann, F., Schmidt, H. J., Nayeri, C. and Paschereit, O. (2015). Drag reduction using base flaps combined with vortex generators and fluidic oscillators on a bluff body. *SAE Int. J. Commercial Vehicles* **8**, **2015-01-2890**, 705–712.

Jönsson, M., Wagner, C. and Loose, S. (2014). Particle image velocimetry of the underfloor flow for generic high-speed train models in a water towing tank. *Proc. Institution of Mechanical Engineers, Part F: J. Rail and Rapid Transit* **228**, **2**, 194–209.

Koenig, K. and Roshko, A. (1985). An experimental study of geometrical effects on the drag and flow field of two bluff bodies separated by a gap. *J. Fluid Mechanics*, **156**, 167–204.

KONVOI Project (2016). http://www.ika.rwth-aachen.de/de/forschung/projekte/fahrerassistenz-und-fahrzeugf%C3%BChrung/1635-konvoi.html, Accessed on May 12, 2016.

Lammert, M. P., Duran, A., Diez, J., Burton, K. and Nicholson, A. (2014). Effect of platooning on fuel consumption of class 8 vehicles over a range of speeds, following distances, and mass. National Renewable Energy Lab. (NREL). Report No. 2014-01-2438.

Larsson, L., Hammar, L., Nilsson, L. U., Berndtsson, A., Knutson, K. and Danielson, H. (1989). A study of ground simulation-correlation between wind-tunnel and water-basin tests of a full scale car. *SAE Trans*., 421–446.

Mason, W. T. and Beebe, P. S. (1978). The Drag Related Flow Field Characteristics of Trucks and Buses. *Aerodynamic Drag Mechanisms of Bluff Bodies and Road Vehicles* (pp. 45–93). Springer. Boston, Massachusetts, USA.

McAuliffe, B. R. and Ahmadi-Baloutaki, M. (2018). A wind-tunnel investigation of the influence of separation distance, lateral stagger, and trailer configuration on the drag-reduction potential of a two-truck platoon. *SAE Int. J. Commercial Vehicles* **11**, **2**, 125–150.

Nayeri, C. N., Glas, J. and Paschereit, C. O. (2010). Towing tank experiments for bluff body aerodynamics. *Engineering Conf. Int. (ECI)*, Potsdam, Germany.

PATH Project (2016). http://www.path.berkeley.edu/research/automated-and-connected-vehicles/truck-platooning, Accessed on May 12, 2016.

Patten, J., McAuliffe, B., Mayda, W. and Tanguay, B. (2012). Review of aerodynamic drag reduction devices for heavy trucks and buses. NRC-CNRC, Report No. CSTT-HVC-TR-205.

Porth, D. and Krämer, W. (1991). Fahrwiderstandsreduzierende massnahmen zur weiteren optimierung der wirtschaftlichkeit von sattelzuegen-teil 2. *Automobiltechnische Zeitschrift* **93**, **10**, 634–640.

Porth, D. and Krämer, W. (1993). Verringerung des verlustleistungspotentials bei nutzfahrzeugen. *Automobiltechnische Zeitschrift* **95**, **12**, 642–649.

Schmidt, H. J., Woszidlo, R., Nayeri, C. N. and Paschereit, C. O. (2015). Drag reduction on a rectangular bluff body with base flaps and fluidic oscillators. *Experiments in Fluids* **56**, **7**, 1–16.

Schmidt, H. J., Woszidlo, R., Nayeri, C. N. and Paschereit, C. O. (2016). Fluidic oscillators for bluff body drag reduction in water. *54th AIAA Aerospace Sciences Meeting*. San Diego, California, USA.

Schmidt, H. J., Woszidlo, R., Nayeri, C. N. and Paschereit, C. O. (2018). The effect of flow control on the wake dynamics of a rectangular bluff body in ground proximity. *Experiments in Fluids* **59**, **6**, 1–16.

Törnell, J., Sebben, S. and Elofsson, P. (2021). Experimental investigation of a two-truck platoon considering inter-vehicle distance, lateral offset and yaw. *J. Wind Engineering and Industrial Aerodynamics*, **213**, 104596.

Tsugawa, S., Kato, S. and Aoki, K. (2011). An automated truck platoon for energy saving. *IEEE/RSJ Int. Conf. Intelligent Robots and Systems (IROS)*, San Francisco, California, USA.

Wabash National (2020). http://www.wabashnational.com, Accessed on November 23, 2020.

WABCO (2020). http://www.wabco-auto.com, Accessed on November 23, 2020.

Watkins, S., Saunders, J. W. and Hoffmann, P. H. (1993). Comparison of road and wind-tunnel drag reductions for commercial vehicles. *J. Wind Engineering and Industrial Aerodynamics* **49**, **1-3**, 411–420.